Mixed finite elements for port-Hamiltonian models of von Kármán beams

Andrea Brugnoli [*] **Ramy Rashad** [*] **Federico Califano** [*]
Stefano Stramigioli [*] **Denis Matignon** [**]

[*] *University of Twente, Enschede, The Netherlands.*
a.brugnoli@utwente.nl, s.stramigioli@utwente.nl
[**] *ISAE-SUPAERO, Université de Toulouse, France.*
denis.matignon@isae.fr

Abstract: A port-Hamiltonian formulation of von Kármán beams is presented. The variables selection lead to a non linear interconnection operator, while the constitutive laws are linear. The model can be readily discretized by exploiting a coenergy formulation and a mixed finite element method. The mixed formulation does not demand the H^2 regularity requirement typical of standard Galerkin discretization of thin structures. A numerical test is performed to assess the convergence rate of the solution.

1. INTRODUCTION

Linear elastic structures have been largely investigated into the port-Hamiltonian (pH) framework as well as the heat equation (consult for instance Macchelli and Melchiorri (2004) for the Timoshenko beam, Aoues et al. (2017) for the Euler-Bernoulli beam, Brugnoli et al. (2019b,a) for thick and thin plates). Recently, more complicated models arising from fluid dynamics have also been considered (Cardoso-Ribeiro et al., 2019, 2020; Rashad et al., 2021a,b; Califano et al., 2021; Altmann and Schulze, 2017).

The Hamiltonian foundation of non-linear elasticity dates back to the late 80s (Simo et al., 1988). A pH formulation of flexible beams undergoing large deformations can be found in Macchelli et al. (2007, 2009). One fundamental non linear theory is the von Kármán one, that applies for moderately large deformation of beams, plates and shells. This theory has puzzled mathematicians and physicists as the derivation of the model rely on some not well justified assumptions. Mathematical conditions under which this theory is actually applicable and will give reasonable results when solved are discussed in Ciarlet (1980, 1990). In particular, for this model the stresses-strains constitutive relation has to be linear and the Kirchhoff-Love displacement field assumption (i.e. the normals to the middle surface remain normal to the deformed middle surface) hold. Existence and uniqueness of solutions for the full dynamical problem were established in Lagnese and Leugering (1991) for one-dimensional beams and in Puel and Tucsnak (1996) for plates. Since the full dynamical von Kárman problem is conservative (see e.g. Bilbao et al. (2015)), a pH realization of this system exists.

The development of new models within the pH framework has been accompanied with an increased interest in numerical discretization methods, capable of retaining the main features of the distributed system in its finite-dimensional counterpart (see Rashad et al. (2020) for a comprehensive review on this topic). Recently, it has become evident that there is a strict link between discretization of port-Hamiltonian systems and mixed finite elements (Cardoso-Ribeiro et al., 2021). An example of this connection is given in Kirby and Kieu (2015), where a velocity-stress formulation for the wave dynamics is shown to be Hamiltonian and its mixed discretization preserves such a structure.

In this contribution, the von Kármán beam model is formulated as a pH system. The selection of energy variables will be such to make the Hamiltonian quadratic in these variables. As a consequence of this choice, the non linearities of the model are included in the interconnection operator, whereas the constitutive relations remain linear. The obtained model can be discretized using mixed finite elements. To this aim, a weak formulation that does not demand for H^2 regularity for the vertical displacement (as in classical Galerkin discretization of beams and plates, cf. Gustafsson et al. (2018)) is obtained. This means that the vertical displacement can be discretized using H^1 conforming elements (i.e. Continuous Galerkin elements), rather then using the more computationally demanding H^2 conforming elements, like the Hermite polynomials. A numerical test is carried out to evaluate the convergence rate of the discrete solution with respect to an analytical one.

The paper is organized as follows. In Section 2 the classical model for von Kármán beams is recalled. Then, a pH realization of the classical model is detailed in Sec. 3. The mixed finite element discretization strategy is discussed in Sec. 4. In Sec. 5 a numerical convergence test is performed to assess the rate of convergence of the solution.

2. VON KÁRMÁN BEAMS

The classical von Kármán beam model is presented in (Reddy, 2010, Chapter 4). Under the hypothesis of isotropic material, the extensional-bending stiffness is zero when the x-axis is taken along the geometric centroidal axis. This means that a pure traction (bending) deformation produces no bending (traction) stress. With this assumption, the problem, defined on an interval $\Omega = [0, L]$, takes the following form

$$
\begin{aligned}
\rho A \ddot{u} &= \partial_x n_{xx}, \\
\rho A \ddot{w} &= -\partial_{xx}^2 m_{xx} + \partial_x(n_{xx}\partial_x w),
\end{aligned}
\tag{1}
$$

together with the stresses and strains expressions

$$
\begin{aligned}
n_{xx} &= EA\varepsilon_{xx}, & m_{xx} &= EI\kappa_{xx}, \\
\varepsilon_{xx} &= \partial_x u + 1/2(\partial_x w)^2, & \kappa_{xx} &= \partial_{xx}^2 w.
\end{aligned}
\tag{2}
$$

Variable u is the horizontal displacement, w is the vertical displacement (cf. Fig. 1), n_{xx} is the axial stress resultant and m_{xx} is the bending stress resultant. The coefficients ρ, A, E, I are the beam's mass density, the cross section, the Young modulus and the second moment of area.
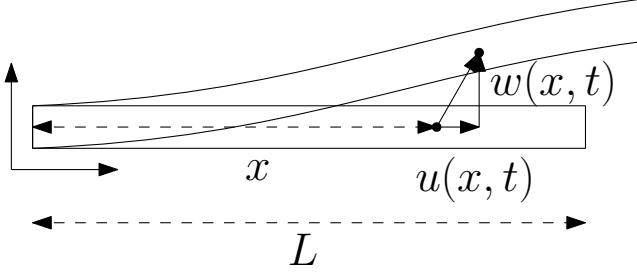

Fig. 1. Schematic representation of a von Kármán beam

The total energy of the model (Hamiltonian functional)

$$
H = \frac{1}{2} \int_\Omega \left\{ \rho A(\dot{u}^2 + \dot{w}^2) + n_{xx}\varepsilon_{xx} + m_{xx}\kappa_{xx} \right\} \, d\Omega,
\tag{3}
$$

consists of the kinetic energy and both membrane and bending deformation energies. This model proves conservative, see Bilbao et al. (2015). Indeed, this implies that a port-Hamiltonian realization of the system exists. We shall demonstrate how to construct a port-Hamiltonian realization, equivalent to (1).

3. THE EQUIVALENT PORT-HAMILTONIAN REALIZATION

To find a suitable port-Hamiltonian system, we first select a set of new energy variables to make the Hamiltonian functional quadratic

$$
\begin{aligned}
\alpha_u &= \rho A \dot{u}, & &\text{Horizontal momentum,} \\
\alpha_\varepsilon &= \varepsilon_{xx}, & &\text{Axial strain,} \\
\alpha_w &= \rho A \dot{w}, & &\text{Vertical momentum,} \\
\alpha_\kappa &= \kappa_{xx}, & &\text{Curvature.}
\end{aligned}
\tag{4}
$$

The energy is quadratic in these variables

$$
H = \frac{1}{2} \int_\Omega \left\{ \frac{\alpha_u^2 + \alpha_w^2}{\rho A} + EA\alpha_\varepsilon^2 + EI\alpha_\kappa^2 \right\} \, d\Omega.
\tag{5}
$$

By computing the variational derivative of the Hamiltonian, one obtains the so-called coenergy variables:

$$
\begin{aligned}
e_u &:= \delta_{\alpha_u} H = \dot{u}, & e_\varepsilon &:= \delta_{\alpha_\varepsilon} H = n_{xx}, \\
e_w &:= \delta_{\alpha_w} H = \dot{w}, & e_\kappa &:= \delta_{\alpha_\kappa} H = m_{xx}.
\end{aligned}
\tag{6}
$$

Before stating the final formulation, consider the unbounded operator operator $\mathcal{C}(w)(\cdot) : L^2(\Omega) \to L^2(\Omega)$, that acts as follows

$$
\mathcal{C}(w)(\cdot) = \partial_x(\cdot\,\partial_x w).
\tag{7}
$$

The domain of the operator is given by

$$
D(\mathcal{C}) = \{v \mid v\,\partial_x w \in H^1(\Omega)\}.
\tag{8}
$$

Proposition 1. The formal adjoint of the $\mathcal{C}(w)(\cdot)$ is given by

$$
\mathcal{C}(w)^*(\cdot) = -\partial_x(\cdot)\partial_x(w).
\tag{9}
$$

Proof 1. Consider a smooth scalar fields with compact support $\psi \in C_0^\infty(\Omega)$ and $\xi \in C_0^\infty(\Omega)$. The formal adjoint of $\mathcal{C}(w)(\cdot)$ satisfies the relation

$$
\langle \psi, \mathcal{C}(w)(\xi) \rangle_\Omega = \langle \mathcal{C}(w)^*(\psi), \xi \rangle_\Omega,
\tag{10}
$$

where $\langle f, g \rangle_\Omega = \int_\Omega fg \, d\Omega$. The proof follows from the computation

$$
\begin{aligned}
\langle \psi, \mathcal{C}(w)(\xi) \rangle_\Omega &= \langle \psi, \partial_x(\xi\,\partial_x w) \rangle_\Omega, \\
&= \langle -\partial_x\psi, \xi\partial_x w \rangle_\Omega, \\
&= \langle -\partial_x\psi\,\partial_x w, \xi \rangle_\Omega.
\end{aligned}
\tag{11}
$$

This means that

$$
\mathcal{C}(w)^*(\cdot) = -\partial_x(\cdot)\partial_x w,
\tag{12}
$$

leading to the final result.

The pH realization is then given by the following system

$$
\frac{\partial}{\partial t}
\begin{pmatrix} \alpha_u \\ \alpha_\varepsilon \\ \alpha_w \\ \alpha_\kappa \end{pmatrix}
=
\begin{bmatrix}
0 & \partial_x & 0 & 0 \\
\partial_x & 0 & (\partial_x w)\,\partial_x & 0 \\
0 & \partial_x(\cdot\,\partial_x w) & 0 & -\partial_{xx}^2 \\
0 & 0 & \partial_{xx}^2 & 0
\end{bmatrix}
\begin{pmatrix} e_u \\ e_\varepsilon \\ e_w \\ e_\kappa \end{pmatrix}.
\tag{13}
$$

The second line of system (13) represents the time derivative of the axial strain ε_{xx}. To close the system, variable w has to be accessible. For this reason, its dynamics has to be included. The augmented system reads

$$
\frac{\partial}{\partial t}
\begin{pmatrix} \alpha_u \\ \alpha_\varepsilon \\ \alpha_w \\ \alpha_\kappa \\ w \end{pmatrix}
=
\underbrace{
\begin{bmatrix}
0 & \partial_x & 0 & 0 & 0 \\
\partial_x & 0 & (\partial_x w)\,\partial_x & 0 & 0 \\
0 & \partial_x(\cdot\,\partial_x w) & 0 & -\partial_{xx}^2 & -1 \\
0 & 0 & \partial_{xx}^2 & 0 & 0 \\
0 & 0 & 1 & & 0
\end{bmatrix}
}_{\mathcal{J}}
\begin{pmatrix} e_u \\ e_\varepsilon \\ e_w \\ e_\kappa \\ \delta_w H \end{pmatrix}.
\tag{14}
$$

The operator $\mathcal{J}$ is formally skew-adjoint. If only the kinetic and deformation energies are considered, it holds $\delta_w H = 0$. In general this term allows accommodation of other potentials, such as gravitational. Suitable boundary variables are then obtained considering the power balance

$$
\dot{H} = \langle e_u, e_\varepsilon \rangle_{\partial\Omega} + \langle e_w, e_\varepsilon\partial_x w - \partial_x e_\kappa \rangle_{\partial\Omega} + \langle \partial_x e_w, e_\kappa \rangle_{\partial\Omega}.
\tag{15}
$$

For the boundary terms, the following notation has been used

$$
\langle f, g \rangle_{\partial\Omega} = fg\big|_0^L = f(L)g(L) - f(0)g(0).
$$

The boundary conditions, summarized in Table 1, are consistent with the ones assumed in Puel and Tucsnak (1996) for deriving a global existence result for this model.

BCs	Traction	Bending	
Dirichlet BCs.	$e_u\|_0^L$	$e_w\|_0^L$	$\partial_x e_w\|_0^L$
Neumann BCs.	$e_\varepsilon\|_0^L$	$e_\varepsilon\partial_x w - \partial_x e_\kappa\|_0^L$	$e_\kappa\|_0^L$

Table 1. Boundary conditions for von Karman beams.

4. MIXED FINITE ELEMENT DISCRETIZATION

To perform the numerical discretization, the constitutive relations are first incorporated in the dynamics. The link between the energy variables (4) and the coenergy variables (6) is given by the linear transformation

$$\begin{pmatrix} \alpha_u \\ \alpha_\varepsilon \\ \alpha_w \\ \alpha_\kappa \end{pmatrix} = \begin{bmatrix} \rho A & 0 & 0 & 0 \\ 0 & C_a & 0 & 0 \\ 0 & 0 & \rho A & 0 \\ 0 & 0 & 0 & C_b \end{bmatrix} \begin{pmatrix} e_u \\ e_\varepsilon \\ e_w \\ e_\kappa \end{pmatrix}, \qquad (16)$$

where $C_a = (EA)^{-1}$ and $C_b = (EI)^{-1}$ are the axial and bending compliances respectively. The physical parameters are assumed to be constant for simplicity. A pure coenergy formulation can then be employed once (16) is plugged into (14)

$$\begin{pmatrix} \rho A \dot{e}_u \\ C_a \dot{e}_\varepsilon \\ \rho A \dot{e}_w \\ C_b \dot{e}_\kappa \\ \dot{w} \end{pmatrix} = \begin{bmatrix} 0 & \partial_x & 0 & 0 & 0 \\ \partial_x & 0 & \partial_x w \, \partial_x & 0 & 0 \\ 0 & \partial_x(\cdot \partial_x w) & 0 & -\partial_{xx}^2 & -1 \\ 0 & 0 & \partial_{xx}^2 & 0 & 0 \\ 0 & 0 & 1 & 0 & 0 \end{bmatrix} \begin{pmatrix} e_u \\ e_\varepsilon \\ e_w \\ e_\kappa \\ \delta_w H \end{pmatrix}. \qquad (17)$$

To derive the discrete system, first (17) is put into weak form. To this aim the test functions $(\psi_u, \psi_\varepsilon, \psi_w, \psi_\kappa, \psi)$ are introduced. For sake of simplicity, no dependency between the displacements and the energy is considered, i.e. $\delta_w H = 0$:

$$\begin{aligned} \langle \psi_u, \rho A \, \dot{e}_u \rangle_\Omega &= \langle \psi_u, \partial_x e_\varepsilon \rangle_\Omega. \\ \langle \psi_\varepsilon, C_a \, \dot{e}_\varepsilon \rangle_\Omega &= \langle \psi_\varepsilon, \partial_x e_u \rangle_\Omega + \langle \psi_\varepsilon, (\partial_x w) \, \partial_x e_w \rangle_\Omega, \\ \langle \psi_w, \rho A \dot{e}_w \rangle_\Omega &= \langle \psi_w, \partial_x(e_\varepsilon \partial_x w) \rangle_\Omega - \langle \psi_w, \partial_{xx}^2 e_\kappa \rangle_\Omega, \\ \langle \psi_\kappa, C_b \, \dot{e}_\kappa \rangle_\Omega &= \langle \psi_\kappa, \partial_{xx}^2 e_w \rangle_\Omega, \\ \langle \psi, \dot{w} \rangle_\Omega &= \langle \psi, e_w \rangle_\Omega. \end{aligned} \qquad (18)$$

Then the integration by parts is performed on the first, third and fourth line. This choice is such to retain the skew-symmetric structure at the discrete level and to lower the regularity requirement for the finite elements (Brugnoli, 2020, Chap. 8). The weak formulation then looks for $(e_u, e_w, e_\kappa, w) \in H^1(\Omega)$, $e_\varepsilon \in L^2(\Omega)$ such that the following system

$$\begin{aligned} \langle \psi_u, \rho A \, \dot{e}_u \rangle_\Omega &= -\langle \partial_x \psi_u, e_\varepsilon \rangle_\Omega + \langle \psi_u, e_\varepsilon \rangle_{\partial\Omega}. \\ \langle \psi_\varepsilon, C_a \, \dot{e}_\varepsilon \rangle_\Omega &= \langle \psi_\varepsilon, \partial_x e_u \rangle_\Omega + \langle \psi_\varepsilon, \partial_x w \, \partial_x e_w \rangle_\Omega, \\ \langle \psi_w, \rho A \dot{e}_w \rangle_\Omega &= -\langle \partial_x \psi_w \partial_x w, e_\varepsilon \rangle_\Omega + \langle \partial_x \psi_w, \partial_x e_\kappa \rangle_\Omega \\ &\quad + \langle \psi_w, e_\varepsilon \partial_x w - \partial_x e_\kappa \rangle_{\partial\Omega}, \\ \langle \psi_\kappa, C_b \, \dot{e}_\kappa \rangle_\Omega &= -\langle \partial_x \psi_\kappa, \partial_x e_w \rangle_\Omega + \langle \psi_\kappa, \partial_x e_w \rangle_{\partial\Omega}, \\ \langle \psi, \dot{w} \rangle_\Omega &= \langle \psi, e_w \rangle_\Omega. \end{aligned} \qquad (19)$$

holds $\forall (\psi_u, \psi_w, \psi_\kappa, \psi) \in H^1(\Omega)$, $\forall \psi_\varepsilon \in L^2(\Omega)$. In this formulation, the boundary axial forces $e_\varepsilon|_0^L$, vertical forces $e_\varepsilon \partial_x w - \partial_x e_\kappa|_0^L$ and rotations $\partial_x e_w|_0^L$ are enforced weakly. To obtain the associated finite-dimensional system, the following Galerkin approximation is considered

$$\begin{aligned} e_u^h &= \sum_{i=1}^{n_u} \xi_u^i(x) e_u^i(t), & \psi_u^h &= \sum_{i=1}^{n_u} \xi_u^i(x) \psi_u^i, \\ e_\varepsilon^h &= \sum_{i=1}^{n_\varepsilon} \xi_\varepsilon^i(x) e_\varepsilon^i(t), & \psi_\varepsilon^h &= \sum_{i=1}^{n_\varepsilon} \xi_\varepsilon^i(x) \psi_\varepsilon^i, \\ e_w^h &= \sum_{i=1}^{n_w} \xi_w^i(x) e_w^i(t), & \psi_w^h &= \sum_{i=1}^{n_w} \xi_w^i(x) \psi_w^i, \qquad (20) \\ e_\kappa^h &= \sum_{i=1}^{n_\kappa} \xi_\kappa^i(x) e_\kappa^i(t), & \psi_\kappa^h &= \sum_{i=1}^{n_\kappa} \xi_\kappa^i(x) \psi_\kappa^i, \\ w^h &= \sum_{i=1}^{n_w} \xi_w^i(x) w^i(t), & \psi^h &= \sum_{i=1}^{n_w} \xi_w^i(x) \psi^i. \end{aligned}$$

Notice that w, e_w are discretized using the same test functions $\xi_w^i(x)$. Plugging (20) into (19), the following finite dimensional system is obtained

$$\begin{pmatrix} \mathbf{M}_u \dot{\mathbf{e}}_u \\ \mathbf{M}_\varepsilon \dot{\mathbf{e}}_\varepsilon \\ \mathbf{M}_w \dot{\mathbf{e}}_w \\ \mathbf{M}_\kappa \dot{\mathbf{e}}_\kappa \\ \dot{\mathbf{w}} \end{pmatrix} = \begin{bmatrix} \mathbf{0} & -\mathbf{D}_{\varepsilon u}^\top & \mathbf{0} & \mathbf{0} \\ \mathbf{D}_{\varepsilon u} & \mathbf{0} & \mathbf{D}_{\varepsilon w}(\mathbf{w}) & \mathbf{0} \\ \mathbf{0} & -\mathbf{D}_{\varepsilon w}^\top(\mathbf{w}) & \mathbf{0} & \mathbf{D}_{w\kappa} \\ \mathbf{0} & \mathbf{0} & -\mathbf{D}_{w\kappa}^\top & \mathbf{0} \\ \mathbf{0} & \mathbf{0} & \mathbf{I} & \mathbf{0} \end{bmatrix} \begin{pmatrix} \mathbf{e}_u \\ \mathbf{e}_\varepsilon \\ \mathbf{e}_w \\ \mathbf{e}_\kappa \end{pmatrix}$$
$$+ \begin{bmatrix} \mathbf{B}_u & \mathbf{0} & \mathbf{0} \\ \mathbf{0} & \mathbf{0} & \mathbf{0} \\ \mathbf{0} & \mathbf{B}_w & \mathbf{0} \\ \mathbf{0} & \mathbf{0} & \mathbf{B}_\kappa \\ \mathbf{0} & \mathbf{0} & \mathbf{0} \end{bmatrix} \begin{pmatrix} \mathbf{u}_1 \\ \mathbf{u}_2 \\ \mathbf{u}_3 \end{pmatrix},$$
$$\begin{pmatrix} \mathbf{y}_1 \\ \mathbf{y}_2 \\ \mathbf{y}_3 \end{pmatrix} = \begin{bmatrix} \mathbf{B}_u^\top & \mathbf{0} & \mathbf{0} & \mathbf{0} \\ \mathbf{0} & \mathbf{0} & \mathbf{B}_w^\top & \mathbf{0} \\ \mathbf{0} & \mathbf{0} & \mathbf{0} & \mathbf{B}_\kappa^\top \end{bmatrix} \begin{pmatrix} \mathbf{e}_u \\ \mathbf{e}_\varepsilon \\ \mathbf{e}_w \\ \mathbf{e}_\kappa \end{pmatrix}. \qquad (21)$$

The fifth entry in the coenergy variables column disappear because $\delta_w H = 0$. The mass matrices are defined as follows

$$\begin{aligned} M_u^{ij} &= \langle \xi_u^i, \rho A \xi_u^j \rangle_\Omega, & M_w^{ij} &= \langle \xi_w^i, \rho A \xi_w^j \rangle_\Omega, \\ M_\varepsilon^{ij} &= \langle \xi_\varepsilon^i, C_a \xi_\varepsilon^j \rangle_\Omega, & M_\kappa^{ij} &= \langle \xi_\kappa^i, C_b \xi_\kappa^j \rangle_\Omega. \end{aligned} \qquad (22)$$

The interconnection matrices are given by

$$\begin{aligned} D_{\varepsilon u}^{ij} &= \langle \xi_\varepsilon^i, \partial_x \xi_u^j \rangle_\Omega, \\ D_{\varepsilon w}^{ij}(\mathbf{w}) &= \left\langle \xi_\varepsilon^i, \sum_{k=1}^{n_w} \partial_x \xi_w^k(x) w^k(t) \partial_x \xi_w^j \right\rangle_\Omega, \qquad (23) \\ D_{w\kappa}^{ij} &= \langle \partial_x \xi_w^i, \partial_x \xi_\kappa^j \rangle_\Omega. \end{aligned}$$

The boundary matrices and control inputs are given by

$$\begin{aligned} B_u^i &= [\psi_u^i(L) \quad \psi_u^i(0)], \\ B_w^i &= [\psi_w^i(L) \quad \psi_w^i(0)], \\ B_\kappa^i &= [\psi_\kappa^i(L) \quad \psi_\kappa^i(0)], \qquad (24) \\ \mathbf{u}_1 &= [e_\varepsilon(L) \quad -e_\varepsilon(0)]^\top, \\ \mathbf{u}_2 &= [e_\varepsilon \partial_x w - \partial_x e_\kappa(L) \quad -e_\varepsilon \partial_x w - \partial_x e_\kappa(0)]^\top, \\ \mathbf{u}_3 &= [\partial_x e_w(L) \quad -\partial_x e_w(L)]^\top. \end{aligned}$$

The outputs $\mathbf{y}_i$ are easily identified thanks to power balance (15), as they corresponds to the power collocated variables w.r.t. the inputs. The discrete energy definition is given by the mass matrices weighted inner product of the coenergy variable

$$H_d = \frac{1}{2}(\mathbf{e}_u \mathbf{M}_u \mathbf{e}_u + \mathbf{e}_\varepsilon \mathbf{M}_\varepsilon \mathbf{e}_\varepsilon + \mathbf{e}_w \mathbf{M}_w \mathbf{e}_w + \mathbf{e}_\kappa \mathbf{M}_\kappa \mathbf{e}_\kappa). \quad (25)$$

The energy rate is computed taking into account the lossless dynamics of System (21) and the discrete energy definition (25):

$$\dot{H}_d = \sum_{i=1}^{3} \mathbf{y}_i^\top \mathbf{u}_i. \quad (26)$$

For the numerical study in Sec. 5, homogeneous boundary conditions will be considered for simplicity.

For what concerns the choice of the underlying finite elements, a simple selection conforming to the weak form (19) is given by continuous Galerkin to discretize the space $H^1(\Omega)$ and discontinuous Galerkin for the space $L^2(\Omega)$. Consider an interval mesh $\mathcal{I}_h$ with elements E. The space of polynomials of order k on a mesh cell is denoted by P_k. The following conforming families of finite elements are selected for this problem:

$$\begin{aligned}
\mathcal{E}_u^h &= \left\{ e_u^h \in H^1(\Omega) | \forall E \in \mathcal{I}_h, \ e_u^h|_E \in P_{2k-1} \right\}, \\
\mathcal{E}_\varepsilon^h &= \left\{ e_\varepsilon^h \in L^2(\Omega) | \forall E \in \mathcal{I}_h, \ e_\varepsilon^h|_E \in P_{2k-2} \right\}, \\
\mathcal{E}_w^h &= \left\{ e_w^h \in H^1(\Omega) | \forall E \in \mathcal{I}_h, \ e_w^h|_E \in P_k \right\}, \\
\mathcal{E}_\kappa^h &= \left\{ e_\kappa^h \in H^1(\Omega) | \forall E \in \mathcal{I}_h, \ e_\kappa^h|_E \in P_k \right\}, \\
\mathcal{W}^h &= \left\{ w^h \in H^1(\Omega) | \forall E \in \mathcal{I}_h, \ w^h|_E \in P_k \right\},
\end{aligned} \quad (27)$$

where $k \geq 1$. The space $\mathcal{E}_u^h$ corresponds to the space of continous Galerkin elements of order $2k - 1$ whereas $\mathcal{E}_w^h, \mathcal{E}_\kappa^h, \mathcal{W}^h$ corresponds to the space of continous Galerkin elements of order k. The space $\mathcal{E}_\varepsilon^h$ corresponds to the space of discontinuous Galerkin elements of order $2k - 2$. This choice guarantees that

$$\begin{aligned}
\partial_x \mathcal{E}_u^h &\subset \mathcal{E}_\varepsilon^h, \\
\partial_x \mathcal{W}^h \cdot \partial_x \mathcal{E}_w^h &\subset \mathcal{E}_\varepsilon^h.
\end{aligned} \quad (28)$$

So the discrete weak formulation becomes: find

$$(e_u^h, \ e_\varepsilon^h, \ e_w^h, \ e_\kappa^h, \ w^h) \in \mathcal{E}_u^h \times \mathcal{E}_\varepsilon^h \times \mathcal{E}_w^h \times \mathcal{E}_\kappa^h \times \mathcal{W}^h$$

such that system (19) holds

$$\forall (\psi_u^h, \ \psi_\varepsilon^h, \ \psi_w^h, \ \psi_\kappa^h, \ \psi^h) \in \mathcal{E}_u^h \times \mathcal{E}_\varepsilon^h \times \mathcal{E}_w^h \times \mathcal{E}_\kappa^h \times \mathcal{W}^h.$$

.

5. NUMERICAL TEST

In this section the convergence rate of the underlying finite elements is assessed by means of a numerical test. A manufactured solution is considered in order to compare the numerical with an analytical manufactured one.

Consider the following manufactured solution for the axial and vertical displacement

$$\begin{aligned}
u^{\text{ex}} &= x^3[1 - (x/L)^3] \sin(2\pi t), \\
w^{\text{ex}} &= \sin(\pi x/L) \sin(2\pi t),
\end{aligned} \quad (29)$$

together with the boundary conditions

$$u|_0^L = 0, \quad w|_0^L = 0, \quad m_{xx}|_0^L = 0. \quad (30)$$

For u and w given in (29) to be the solution of (1), appropriate forcing terms have to be introduced in the right hand side of (1). These are given by

$$\begin{aligned}
f_u &= \rho A \partial_{tt}^2 u^{\text{ex}} - \partial_x n_{xx}^{\text{ex}}, \\
f_w &= \rho A \partial_{tt}^2 w^{\text{ex}} + \partial_{xx}^2 m_{xx}^{\text{ex}} - \partial_x (n_{xx}^{\text{ex}} \partial_x w^{\text{ex}}),
\end{aligned} \quad (31)$$

The forcing term are computed considering the projection of the analytical forcing terms on the corresponding test functions ψ_u, ψ_w. Given the finite element selection (27), this test function corresponds to the Lagrange elements of order $2k - 1$ and k for ψ_u and ψ_w respectively.

The numerical values of the parameters for the simulation are reported in Table 2. The Firedrake library (Rathgeber et al. (2017)) is used to generate the matrices. To integrate the equations in time a Crank-Nicholson scheme is employed. The time step is set to $\Delta t = h/(2\pi)$ to balance the time discretization error with respect to the spatial error. The final time is set to $t_f = 1[\text{s}]$. The non-linear system is solved using Newton-Krylov iterations with a line search and direct factorization of the linear system.

To measure the convergence rate, suitable norms have to be introduced. Let $\mathcal{X}$ be a Hilbert space, and t_f a positive real number. We denote by $L^\infty([0, t_f]; \mathcal{X})$ or $L^\infty(\mathcal{X})$ the space of functions $f : [0, t_f] \to \mathcal{X}$ for which the time-space norm $|| \cdot ||_{L^\infty([0,t_f];\mathcal{X})}$ satisfies

$$||f||_{L^\infty([0,t_f];\mathcal{X})} = \operatorname*{ess\,sup}_{t \in [0,t_f]} ||f||_\mathcal{X} < \infty.$$

To compute the $L^\infty(\mathcal{X})$ space-time dependent norm from the numerical results, the discrete norm $L^\infty_{\Delta t}(\mathcal{X})$ is used

$$|| \cdot ||_{L^\infty(\mathcal{X})} \approx || \cdot ||_{L^\infty_{\Delta t}(\mathcal{X})} = \max_{t \in t_i} || \cdot ||_\mathcal{X},$$

where t_i are the discrete simulation instants. The Hilbert space $\mathcal{X}$ depends on the regularity of the considered variable. For variables (e_u, e_w, e_κ, w) the error is measured in the $L^\infty_{\Delta t}(H^1)$ norm, whereas for e_ε is measured using the $L^\infty_{\Delta t}(L^2)$ norm. The simulation results are reported in Fig. 2. It can be noticed that all variables converge at rate given by the polynomial degree k. For variable e_κ a superconvergent trend can be observed for case $k = 1$ (cf. Fig 2d). The numerical solutions for the different variables is plotted in Fig. 3.

Beam parameters				
E	ρ	L	A	I
70 [kPa]	2700 [kg/m^3]	1 [m]	0.01 [m^2]	8.3 10^{-6} [m^4]

Table 2. Physical parameters for the beam.

6. CONCLUSION

In this contribution, a pH model for von Kármán beams is detailed. The resulting system of equations is then discretized using mixed finite elements. The validity of discretized model is assessed by comparison with an analytical solution. This demonstrates how pH formulations can be used in relevant non linear models arising from engineering. A natural outlook is the extension of this formulation to the two-dimensional case Brugnoli and Matignon (2022).

(a) $L^\infty_{\Delta t}(H^1)$ error for e_u

(b) $L^\infty_{\Delta t}(L^2)$ error for e_ε

(c) $L^\infty_{\Delta t}(H^1)$ error for e_w

(d) $L^\infty_{\Delta t}(H^1)$ error for e_κ

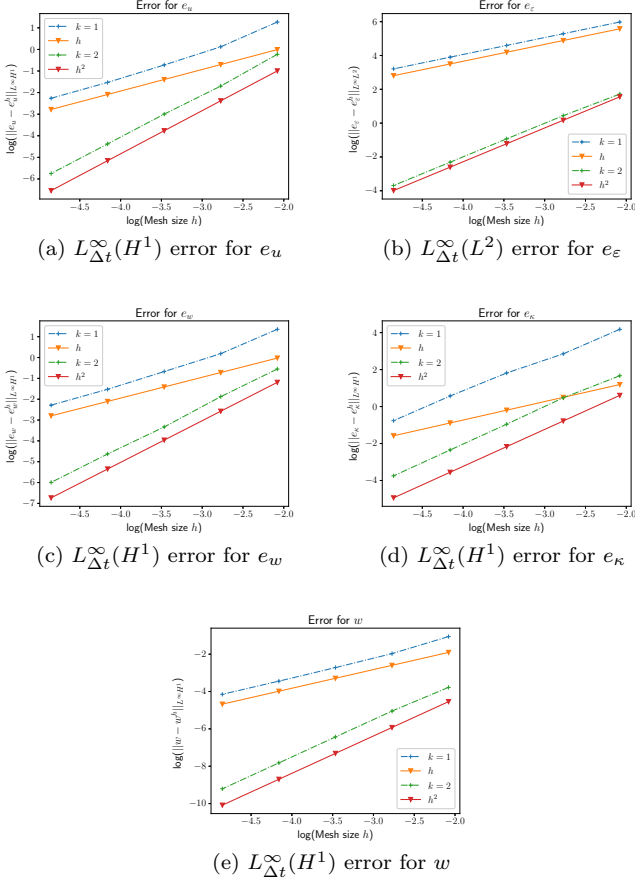(e) $L^\infty_{\Delta t}(H^1)$ error for w

Fig. 2. Error trend for the different variables

The analysis of this model under a control theoretic perspective represents another interesting development. The numerical discrete model can be used to construct model based controllers.

ACKNOWLEDGEMENTS

REFERENCES

R. Altmann and P. Schulze. A port-Hamiltonian formulation of the Navier–Stokes equations for reactive flows. *Systems & Control Letters*, 100:51 – 55, 2017. ISSN 0167-6911. doi: https://doi.org/10.1016/j.sysconle.2016.12.005.

S. Aoues, F.L. Cardoso-Ribeiro, D. Matignon, and D. Alazard. Modeling and control of a rotating flexible spacecraft: a port-Hamiltonian approach. *IEEE Transactions on Control Systems Technology*, 27(1):355–362, 2017.

S. Bilbao, O. Thomas, C. Touzé, and M. Ducceschi. Conservative numerical methods for the full von Kármán plate equations. *Numerical Methods for Partial Differential Equations*, 31(6):1948–1970, 2015. doi: 10.1002/num.21974.

A. Brugnoli. *A port-Hamiltonian formulation of flexible structures. Modelling and structure-preserving finite element discretization.* PhD thesis, Université de Toulouse, ISAE-SUPAERO, France, 2020.
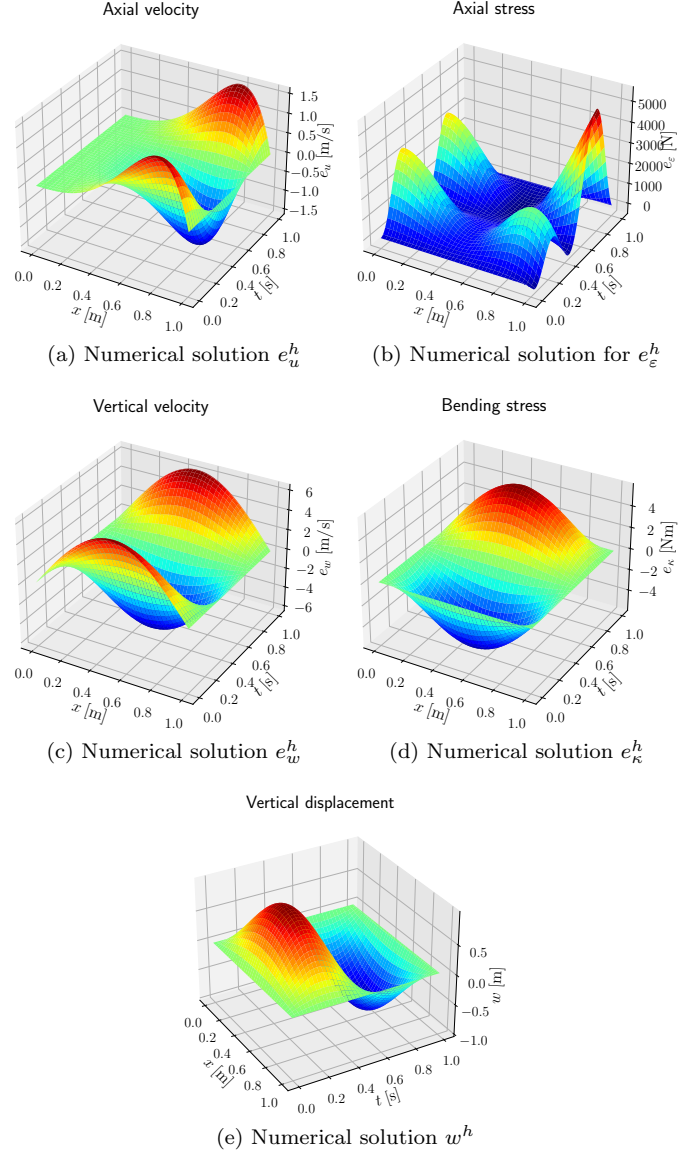
(a) Numerical solution e_u^h

(b) Numerical solution for e_ε^h

(c) Numerical solution e_w^h

(d) Numerical solution e_κ^h

(e) Numerical solution w^h

Fig. 3. Computed numerical solution for $h = 2^{-5}$ and $k = 2$ for the different variables

A. Brugnoli and D. Matignon. A port-Hamiltonian formulation for the full von-Kármán plate model. In *ENOC 2020 - Proceedings of 10th European Nonlinear Dynamics Conference*, 2022.

A. Brugnoli, D. Alazard, V. Budinger, and D. Matignon. Port-Hamiltonian formulation and symplectic discretization of plate models. Part II: Kirchhoff model for thin plates. *Applied Mathematical Modelling*, 75:961–981, 2019a.

A. Brugnoli, D. Alazard, V. Budinger, and D. Matignon. Port-Hamiltonian formulation and symplectic discretization of plate models. Part I: Mindlin model for thick plates. *Applied Mathematical Modelling*, 75:940–960, 2019b.

Federico Califano, Ramy Rashad, Frederic P. Schuller, and Stefano Stramigioli. Geometric and energy-aware decomposition of the navier–stokes equations: A port-hamiltonian approach. *Physics of Fluids*, 33(4):047114, 2021. doi: 10.1063/5.0048359.

F.L. Cardoso-Ribeiro, A. Brugnoli, D. Matignon, and L. Lefèvre. Port-Hamiltonian modeling, discretization

and feedback control of a circular water tank. In *2019 IEEE 58th Conference on Decision and Control (CDC)*, pages 6881–6886. IEEE, 2019.

F.L. Cardoso-Ribeiro, D. Matignon, and V. Pommier-Budinger. Port-Hamiltonian model of two-dimensional shallow water equations in moving containers. *IMA Journal of Mathematical Control and Information*, 37(4):1348–1366, 07 2020. ISSN 1471-6887. doi: 10.1093/imamci/dnaa016.

Flávio Luiz Cardoso-Ribeiro, Denis Matignon, and Laurent Lefèvre. A partitioned finite element method for power-preserving discretization of open systems of conservation laws. *IMA Journal of Mathematical Control and Information*, 38(2):493–533, 6 2021. ISSN 1471-6887. doi: 10.1093/imamci/dnaa038.

P.G. Ciarlet. A justification of the von Kármán equations. *Archive for Rational Mechanics and Analysis*, 73(4): 349–389, Dec 1980. ISSN 1432-0673. doi: 10.1007/BF00247674.

P.G. Ciarlet. *Plates and Junctions in Elastic Multistructures: an Asymptotic Analysis*. Springer-Verlag, 1990.

T. Gustafsson, R. Stenberg, and J. Videman. A posteriori estimates for conforming Kirchhoff plate elements. *SIAM Journal on Scientific Computing*, 40(3):A1386–A1407, 2018. doi: 10.1137/17M1137334.

R.C. Kirby and T.T. Kieu. Symplectic-mixed finite element approximation of linear acoustic wave equations. *Numerische Mathematik*, 130(2):257–291, Jun 2015. ISSN 0945-3245. doi: 10.1007/s00211-014-0667-4.

J.E Lagnese and G. Leugering. Uniform stabilization of a nonlinear beam by nonlinear boundary feedback. *Journal of Differential Equations*, 91(2):355 – 388, 1991. ISSN 0022-0396. doi: https://doi.org/10.1016/0022-0396(91)90145-Y.

A. Macchelli and C. Melchiorri. Modeling and control of the Timoshenko beam. The distributed port Hamiltonian approach. *SIAM Journal on Control and Optimization*, 43(2):743–767, 2004.

A. Macchelli, C. Melchiorri, and S. Stramigioli. Port-based modeling of a flexible link. *IEEE Transactions on Robotics*, 23:650 – 660, Sep 2007. doi: 10.1109/TRO.2007.898990.

A. Macchelli, C. Melchiorri, and S. Stramigioli. Port-based modeling and simulation of mechanical systems with rigid and flexible links. *IEEE Transactions on Robotics*, 25(5):1016–1029, Oct 2009. doi: 10.1109/TRO.2009.2026504.

J.P. Puel and M. Tucsnak. Global existence for the full von Kármán system. *Applied Mathematics and Optimization*, 34(2):139–160, Sep 1996. ISSN 1432-0606. doi: 10.1007/BF01182621.

R. Rashad, F. Califano, A.J. van der Schaft, and S. Stramigioli. Twenty years of distributed port-Hamiltonian systems: a literature review. *IMA Journal of Mathematical Control and Information*, 37(4):1400–1422, 07 2020. ISSN 1471-6887. doi: 10.1093/imamci/dnaa018.

R. Rashad, F. Califano, F.P. Schuller, and S. Stramigioli. Port-Hamiltonian modeling of ideal fluid flow: Part I. foundations and kinetic energy. *Journal of Geometry and Physics*, page 104201, 2021a. ISSN 0393-0440. doi: https://doi.org/10.1016/j.geomphys.2021.104201.

R. Rashad, F. Califano, F.P. Schuller, and S. Stramigioli. Port-Hamiltonian modeling of ideal fluid flow: Part II. compressible and incompressible flow. *Journal of Geometry and Physics*, page 104199, 2021b. ISSN 0393-0440. doi: https://doi.org/10.1016/j.geomphys.2021.104199.

F. Rathgeber, D.A. Ham, L. Mitchell, M. Lange, F. Luporini, A. T.T. McRae, G.T. Bercea, G. R. Markall, and P.H.J. Kelly. Firedrake: automating the finite element method by composing abstractions. *ACM Transactions on Mathematical Software (TOMS)*, 43(3):24, 2017.

J.N. Reddy. *An Introduction to Nonlinear Finite Element Analysis*. Oxford University Press, 2010. doi: https://doi.org/10.1093/acprof:oso/9780198525295.001.0001.

J.C. Simo, J.E. Marsden, and P.S. Krishnaprasad. The Hamiltonian structure of nonlinear elasticity: the material and convective representations of solids, rods, and plates. *Archive for Rational Mechanics and Analysis*, 104(2):125–183, Jun 1988. ISSN 1432-0673. doi: 10.1007/BF00251673.